Radiation Physics and Chemistry 116 (2015) 292–299

Contents lists available at ScienceDirect

Radiation Physics and Chemistry

journal homepage: www.elsevier.com/locate/radphyschem

Dosimetry and image quality in digital mammography facilities in the State of Minas Gerais, Brazil

Sabrina Donato da Silva [a,b,*], Geórgia Santos Joana [b], Bruno Beraldo Oliveira [a,c], Marcio Alves de Oliveira [d], Fernando Leyton [a,e,f], Maria do Socorro Nogueira [a,b]

[a] Post-Graduate in Science and Technology of Radiations, Minerals and Materials – CDTN/CNEN, Belo Horizonte, MG, Brazil
[b] Post-Graduate in Nuclear Science and Technology/Department of Nuclear Energy, Federal University of Minas Gerais-DEN/UFMG, Belo Horizonte, MG, Brazil
[c] Barretos Cancer Hospital/Pio XII Foundation, Barretos, SP, Brazil
[d] Department of Oncology/Clinics Hospital of Uberlândia – UFU, Uberlândia, MG, Brazil
[e] Faculty of Health and Odontology, Diego Portales University, Santiago, Chile
[f] Radiological Sciences Center, Health Sciences Faculty, Tarapacá University, Arica, Chile

HIGHLIGHTS

- Mean glandular dose and image quality in digital mammography systems.
- Linearity of the detector response to the system computed radiography.
- Dosimetry and image quality on digital mammography in Minas Gerais, Brazil.
- 44% Of CR and DR mammography systems passed in the evaluation of mean glandular dose.
- The overall uncertainty for mean glandular dose measurement was 5.2%.

ARTICLE INFO

Article history:
Received 8 October 2014
Received in revised form
9 May 2015
Accepted 12 May 2015
Available online 1 June 2015

Keywords:
Mammography
Mean glandular dose
Quality control
Contrast-to-noise ratio

ABSTRACT

According to the National Register of Health Care Facilities (CNES), there are approximately 477 mammography systems operating in the state of Minas Gerais, Brazil, of which an estimated 200 are digital apparatus using mainly computerized radiography (CR) or direct radiography (DR) systems. Mammography is irreplaceable in the diagnosis and early detection of breast cancer, the leading cause of cancer death among women worldwide. A high standard of image quality alongside smaller doses and optimization of procedures are essential if early detection is to occur. This study aimed to determine dosimetry and image quality in 68 mammography services in Minas Gerais using CR or DR systems. The data of this study were collected between the years of 2011 and 2013. The contrast-to-noise ratio proved to be a critical point in the image production chain in digital systems, since 90% of services were not compliant in this regard, mainly for larger PMMA thicknesses (60 and 70 mm).

Regarding the image noise, only 31% of these were compliant. The average glandular dose found is of concern, since more than half of the services presented doses above acceptable limits. Therefore, despite the potential benefits of using CR and DR systems, the employment of this technology has to be revised and optimized to achieve better quality image and reduce radiation dose as much as possible.

1. Introduction

In recent decades cancer has gained greater prominence, becoming a global public health problem. According to the World Health Organization, in the year 2030 one can expect 27 million incident cases of cancer, with 17 million deaths and 75 million people living with the disease (INCA, 2014). Among the types of cancer, breast cancer is the second most common type in the world and the most common among women, accounting for 22% of new cases each year. Data from the National Cancer Institute reveal that 57,120 new cases of breast cancer are expected in Brazil for the year 2014. In the state of Minas Gerais, Brazil, the estimate is 5210 new cases each year (INCA, 2014).

Mammography is irreplaceable in the diagnosis and early

* Corresponding author.
E-mail address: sadonatosilva@hotmail.com (S.D. da Silva).

http://dx.doi.org/10.1016/j.radphyschem.2015.05.024
0969-806X/© 2015 Published by Elsevier Ltd.

detection of breast cancer. The introduction of digital technologies in mammography, through the computed radiography (CR) and direct digital radiology (DR), has created new expectations for this technique, based on its potential benefits in the early detection of breast cancer. CR systems use phosphor plates and a separate reader. DR systems have an integrated x-ray system and detector. The image is available on the computer immediately after the x-ray exposure (Bick and Diekmann (2009).

There is a small but significant risk of carcinogenesis induced by x-rays in performing a mammogram. However, testing the quality of the technical aspects of mammography equipment at regular time-intervals can minimize this risk. Determination of mean glandular dose (D_G) is an important factor in quality control of mammography systems, since this is the dosimetric quantity that best defines this risk (Dance et al., 1999).

In the European Guidelines (Perry et al., 2006) the image quality is expressed via contrast thresholds. This criterion is evaluated with the Contrast Detail for Mammography (CDMAM) test object (Artinis, the Netherlands). The Artinis CDMAM phantom consists of an aluminum base with gold disks of different thicknesses and diameters, and aims at testing the ability of detecting objects with very small contrast and diameter in mammography. The results of an analysis with the CDMAM phantom are threshold levels expressed as x-ray contrast or in terms of the thickness of gold disks. This analysis is featured by the relationship between the thresholds of visualization of disks and dose values related to that image. This research aimed at evaluating the mean glandular dose to which patients are exposed while undergoing a mammogram using CR or DR systems; image quality was evaluated using images of the CDMAM phantom. The overall uncertainty for mean glandular dose measurement with solid-state dosimeter (Unfors Xi) was estimated at 5.2%.

2. Material and methods

In this study 68 digital processing systems were assessed, including 65 CR systems and 3 DR systems, for a total of 72 combinations of mammography-CR or DR. This corresponds to approximately 14% of mammography units currently in use throughout Minas Gerais and about 34% of digital mammography systems. (Tables 1 and 2). According to the (CNES (2014), there are approximately 477 mammography services operating in Minas Gerais, of which about 200 are digital apparatus using CR or DR systems.

2.1. Image quality for CR or DR systems

It is recognized that high-quality images are essential for the reliable detection in the breast mammography. There is no clear pattern for specifying mammographic image quality (ICRU, 2009). However, knowing to quality of the images depends of several factors like the performance of x-ray unit and image detector (NHSBSP, 2009). Taking into account such allegations, in order to assess the quality of mammographic images and the integration between mammography unit and digital image processing system, besides the analysis of image quality parameters like contrast and definition by means of a breast phantom, the linearity of the detector response, the contrast-to-noise ratio, noise and average glandular dose were evaluated.

Table 1
Mammography systems and mammography DR studied.

Manufacturer of the mammography unit	Percentage of systems assessed
GE	65
Hologic[a]	10
Siemens	13
VMI[b]	7
Other (Philips, Elscint)	5

[a] Three of them were DR systems.
[b] VMI is a mammography unit made in Brazil.

Table 2
CR modalities studied.

Manufacturer of the CR reader	Percentage of systems assessed
KODAK	43
FUJI	39
AGFA	18

2.1.1. Linearity of the detector response

The exposure range over which the detector response is linear could be specified by the manufacturer. In the DR system the mean pixel value (MPV), depending on the values of the incident air kerma (K_i), has a linear response. For CR systems this relation is logarithmic.

In this test, four polymethyl methacrylate (PMMA) plates measuring $18 \times 24\ \text{cm}^2$ with the thickness of 1 cm each were positioned near the output of the x-ray tube to provide the image, and measure the incident air kerma, K_i. The K_i value was measured with a solid-state detector (Unfors Xi R/F & MAM platinum detector, serial number 181096). The generated and used images in the analysis were saved without processing (raw data). These measurements were performed with a x-ray tube voltage of 28 kV, alongside with an anode-filter combination Mo/Mo, and a wide interval of current exposure time product values: 4, 8, 16, 25, 32, 45, 63, 100 and 140 mAs. According to SEFM (2007) the tube voltage of 28 kV and the anode-filter combination Mo/Mo are standard conditions for performing this test. Besides, the response function of the detector is assessed in the manual mode with the range of mAs that cover 1/10 or five times the value of mAs used for radiographing a standard simulator, in this case, we used one with 45 mm of PMMA. In this research the devices tested were very old, and for safety issues it was not spent the given amount of 140 mAs during quality control assessments. For the CR systems, MPV is represented in the function of the logarithm of K_i and is provided by (SEFM, 2012):

$$\text{MPV} = a\ln(K_i) + b \tag{1}$$

where MPV is the mean pixel value, $\ln(K_i)$ is the value of the logarithm of the air kerma and $\boldsymbol{a}$ and $\boldsymbol{b}$ are fitted coefficients of the linear equation. In each image, a region of interest (ROI) of $4\ \text{cm}^2$ was selected at 6 cm from the thorax wall in order to provide the MPVs and standard deviations (SD) of the image.

With the coefficients $\boldsymbol{a}$ and $\boldsymbol{b}$ of the linear equation (Eq. (1)), the MPVs and SDs were linearized through Eqs. (2) and (3) respectively (SEFM, 2012):

$$\text{MPV}' = e^{\left(\frac{\text{MPV}-b}{a}\right)} \tag{2}$$

$$\text{SD}' = \frac{\text{SD}}{a} e^{\left(\frac{\text{MPV}-b}{a}\right)} \tag{3}$$

where MPV′ is the linearized mean pixel value, MPV is the mean pixel value, and $\boldsymbol{a}$ and $\boldsymbol{b}$ are the fitted coefficients of Eq. (1) (SEFM, 2012). In addition to that, SD′ and SD are the values of linearized standard deviation and standard deviation associated with the image background, respectively. For DR systems, the linearization of SD and MPV was not necessary because the system already presents a linear response. If the coefficient of

Table 3
Values minimum, maximum, mode of the kV and mAs used in this research and the anode-filter most used in the test of CNR.

Thickness of PMMA (cm)	Minimum tube voltage (kV)	Maximum tube voltage (kV)	Mode	Minimum tube loading (mAs)	Maximum tube loading (mAs)	Mode	Anode-Filter combination most used
2	22	29	26	5.6	100	36	Mo/Mo
3	24	30	26	9	775	50	Mo/Mo
4	24	31	28	16	207	100	Mo/Mo
5	26	33	29	32	280	110	Mo/Mo
6	28	34	31	45	375	160	Mo/Mo
7	32	35	28	80	600	280	Mo/Mo

determination, R^2, obtained from linear regression of the values of MPV′, in the case of DR systems MPV versus kerma, exceed 0.99, then the detection system has a linear response.

2.1.2. Contrast-to-noise ratio (CNR)

In this test, PMMA plates measuring $18 \times 24\,cm^2$ with thicknesses ranging from 2 to 7 cm were used. Between the first and second bottom plates of PMMA, a 0, 2 mm-thick-aluminum foil measuring 1 cm × 1 cm was inserted laterally centered at 6 cm from the chest wall to create an area of contrast in the image. It is noteworthy that the aluminum plates were positioned in such a way that they do not interfere with the AEC. Exposures for each thickness were performed with automatic exposure control (AEC), followed by registration of these parameters (Table 3). Images were recorded with no processing (raw data) for subsequent analysis. ROIs were chosen according to Fig. 1, with one ROI placed outside the aluminum foil region (background image), and the second ROI over this region.

The MPV′ and SD′ values for each ROI were determined based on Eqs. (2) and (3), and CNR calculated for each breast thickness using Eq. (4) (SEFM, 2012).

$$CNR = \frac{MPV'_{Al} - MPV'_{B}}{\sqrt{(SD'^2_{Al} + SD'^2_{B})/2}} \quad (4)$$

where MPV'_{Al} is the linearized mean pixel value of the region of the aluminum foil; MPV'_B is the linearized mean pixel value of the background image; SD'^2_{Al} is linearized standard deviation within the aluminum foil, and SD'^2_B is the linearized standard deviation of the background. Relative CNR values obtained for each thickness are evaluated based on the reference values of CNR obtained for the thickness of 5 cm of PMMA and based on the cut-off for non-compliance determined by the SEFM 2011 (Table 4) (Oliveira et al., 2011).

2.1.3. Noise

Noise is inherent to digital image, and appears in all stages of its production chain. Noise may be estimated by the standard deviation of the detected signal, namely by the fluctuation in the response of the detection system (Chevalier and Torres, 2010; Bouwman et al., 2009). Detectors may present limitations due to quantum noise in low dose ranges, the structural noise, which is dose-dependent, and electronic noise, which depends only upon the reading and signal amplification. With the test results from the linearity of the detector response, it was built a graph of air kerma by standard deviations linearized and, consequently, determined the type power trend line that best fits to the points of the power curve of the equation ($y = ax^b$) (SEFM, 2012). For DR systems, the graph was made with the air kerma by the standard deviations.

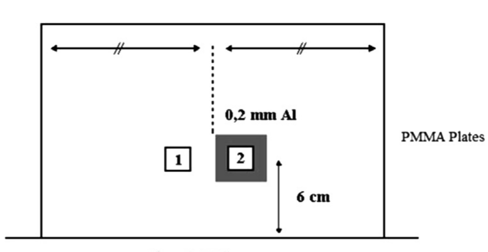

Fig. 1. Position of aluminum foil and ROIs 1 and 2 to evaluate the CNR (SEFM, 2007; Dantas, 2010).

Table 4
CNR limit values for each thick PMMA.

Thickness of PMMA	Threshold for relative CNR (%)
20	>115
30	>110
40	>105
50	>100
60	>95
70	>90

SEFM (2007, 2012).

Power index values (b) close or equal to 0.5 indicate that the largest component of noise is quantum noise. Values greater than 0.5 are associated with the presence of structural noise, while lower values are associated with electronic noise (SEFM, 2012).

2.1.4. Image quality

The quality of the image was assessed using a CDMAM 3.4 phantom (Fig. 2A). The Artinis CDMAM 3.4 phantom (Artinis, 2014) consists of an aluminum base with gold disks (99.99% pure gold) of varying different thickness and diameter. The gold disks are arranged in a matrix of 16 lines by 16 columns. Within a row the disk diameter is constant, with (partly) logarithmic increasing thickness. Within a column the thickness of the disks is constant and the diameter increases logarithmically. The thickness is between 0.03 and 2.00 μm and the diameter is between 0.06 and 2.0 mm. Each square contains two identical disks (equal thickness and diameter), one in the center and one in a randomly chosen corner. The aluminum base (0.5 mm thick Al, 99.5% pure aluminum) is attached to a PMMA cover (3 mm). Under normal mammography-radiation conditions (Mo anode, 30 mm Mo filter, 28 kV), the aluminum base and PMMA cover have a combined equivalent PMMA thickness of 10 mm. The phantom is delivered with 4 PMMA plates, each of 10 mm thickness, which are used for the simulation of different breast thicknesses. Every plate has an engraved marker for identification. The image quality was assessed from the observation of the contrast thresholds by visualizing gold disks in CDMAM phantom. This threshold is defined as being the minimum visualized thickness of gold disk for each simulated breast thickness. Twelve images of CDMAM phantom, with four PMMA plates, were obtained by using semi-automatic exposure control with a tube voltage of 28 kV. After the exposures, the images were assessed automatically using the software (Thijssen et al., 2006) Analyser Software V1.2, provided by the manufacturer. Thus, it was determined the thickness of the disks of 0.10; 0.25; 0.50; 1.00 and 2.00 mm diameter which are in the

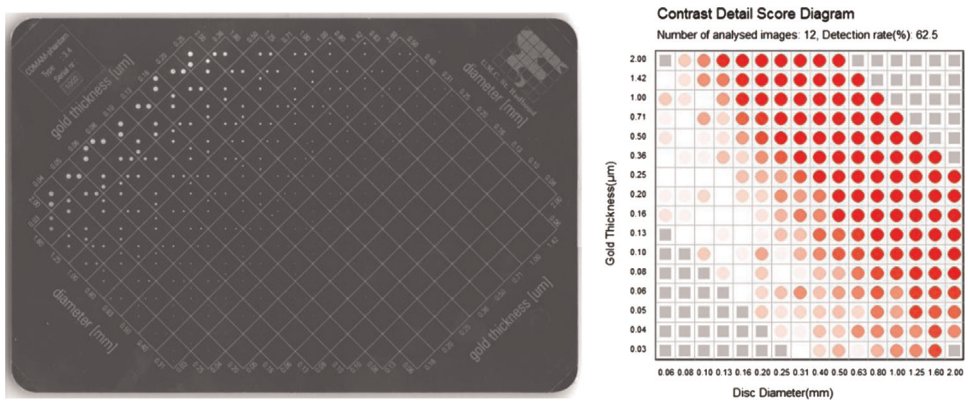

Fig. 2. (A) Phantom CDMAM and (B) contrast detail score diagram (Thijssen et al., 2006). (For interpretation of the references to color in this figure legend, the reader is referred to the web version of this article).

contrast threshold for the images that could be viewed according to the cut off for compliance of the SEFM (2012, 2007).

The software points out in its results report recognized disks in the image, separating those in the center and those in positions outside the central position of the cell. After performing this assessment, the program shows the detailed contrast score that indicates the percentage of correct positions detected (Fig. 2B). In the contrast detail diagram (Fig. 2B) generated by the analysis software CDMAM the cells without gold are displayed with a gray frame, cells with less than 25% or detected with a percentage of 25% are shown in white, cells with 100% of the disks detected are shown entirely red. The other cells are shown somehow red, “pale red” with a color proportional to its detection rate (Thijssen et al., 2006). Table 5 shows the acceptable values of thicknesses of the gold disk that should be viewed for each evaluated gold disk diameter.

2.1.5. Mean glandular dose (D_G)

Incident air kerma (K_i) measurements were conducted according to the Spanish protocol on dosimetry in mammography (SEFM, 2012). K_i and the half value layer were measured automatically using an appropriately calibrated solid-state dosimeter (Unfors Xi). For each exposure, tube potential (kVp) and current exposure time product (mAs) were recorded. Mean glandular dose (D_G) was calculated by applying published conversion factors to the measured K_i values (SEFM, 2012; Oliveira et al., 2014; Dance et al., 2000) from the following equation:

$$D_G = K_i.\, g.\, c.\, s \qquad (5)$$

Where g is the conversion coefficient from K_i to mean glandular dose, corresponding to a glandularity of 50% and depends on the half-value layer (HVL) and breast thickness; s is a factor depending on the anode/filter combination and was equal to one for Mo/Mo and c is the conversion coefficient which corrects for any difference in breast composition from 50% glandularity. Table 6 shows the acceptable values limit of mean glandular dose (SEFM, 2012).

Table 5
Minimum thickness of gold disks that should be displayed for each diameter in CDMAM simulator.

Diameter (mm)	Acceptable values (µm)
0.10	< 1.68
0.25	< 0.352
0.50	< 0.150
1.00	< 0.091
2.00	< 0.069

SEFM (2007, 2012).

Table 6
Mean glandular dose limit values for each thick PMMA.

Thickness (cm)		D_G (mSv)	
PMMA	MAMA equivalent	Acceptable	Desirable
2	2.1	< 1.0	< 0.6
3	3.2	< 1.5	< 1.0
4	4.5	< 2.0	< 1.6
5	6	< 3.0	< 2.4
6	7.5	< 4.5	< 3.6
7	9	< 6.5	< 5.1

SEFM (2007, 2012).

3. Results and discussion

This study evaluated three of the four computed radiography systems in use in Brazil (Agfa, Fuji and Kodak). The average value found for the usage time of digitizing units (CR) was approximately two years. The unit with the longest usage was six years old and the shortest time was one week. 65 mammography systems with various CR manufacturers (Table 2) were examined with respect to dose and image quality. The average time of use for the mammography units was about nine years, in a range from 3 months to 20 years. More than 20 mammography units had more than 10 years of use.

The number of mammograms performed by mammography systems varied from 30 to 1200 per month, with an average of approximately 441 mammograms per month per unit. According to the study by Oliveira et al. (2007) the average number of mammograms performed per month in conventional mammography services in Minas Gerais was 300. According to a study done by (Dantas, 2010), the average was 750 mammograms per month. The increase in the monthly number of mammograms in comparison with the Oliveira study (Oliveira et al., 2007) can be explained by the shorter scan time for a CR or DR image, compared to conventional mammography, which makes use of wet chemistry imaging systems. The lower number of mammograms performed compared to the Dantas study (Dantas, 2010) is due to the larger sample size in this study, which includes towns from the countryside where the number of mammograms is much lower than in the state capital.

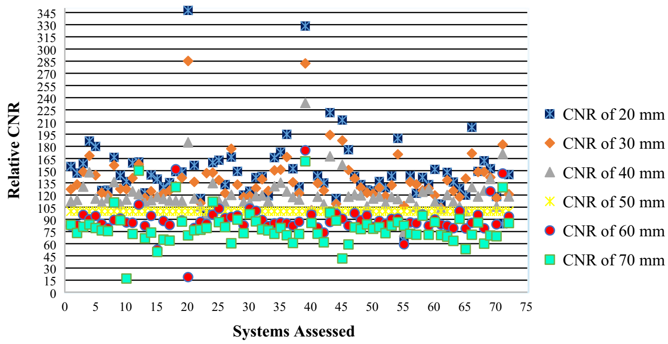

Fig. 3. Dispersion relative CNR found on the evaluation of Contrast-to-noise ratio.

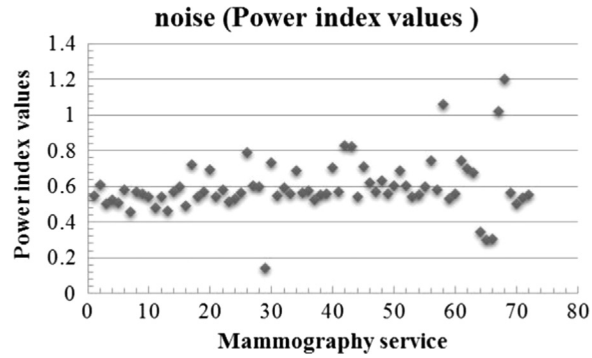

Fig. 4. Dispersion of power index found on evaluation of image noise.

3.1. Linearity of the detector response

From 72 of the mammography systems evaluated, 61 showed a correlation coefficient (R^2) greater than 0.99, corresponding to 85% of compliance (Table 9). Similar result was attained by (Dantas, 2010), where all facilities had R^2 equal to 0.99. One of three DR systems assed failed in this test obtaining R^2 equal to 0.94. From non-compliant services, only two had less than four years of use of the mammography equipment for DR systems, this information was not registered in the reports. It is possible to affirm that length of use of the mammography equipment is linked to non-compliance.

3.2. Contrast-to-noise ratio (CNR)

CNR presents great influence on the image production chain in digital systems. In this study it was found that 65 out of the 72 mammography systems assessed (90%) presented non-compliance on this parameter (Table 9). Fig. 3 shows the dispersion of relative CNR found on the evaluation for each thickness. The minimum and maximum values found for each thickness are showed in Table 7.

A similar result was obtained in the work of Dantas (2010), in which 85% of the evaluated services were considered non-compliant, especially for larger thicknesses of PMMA. However, in this study, all measurements were performed with the CAE, and yet showed unsatisfactory performance evidencing that CR devices were not properly integrated with mammography units, and that DR systems also need to be optimized, since two of the three DR systems evaluated showed non-compliance.

3.3. Noise

Regarding image noise the systems evaluated proved to be problematic, with only 22 mammography-CR combinations obtaining the desired power index between 0.450 and 0.550, equating to 31% compliance (Table 9). For most of the services evaluated, non-compliance was due to the presence of structural noise because the vast majority of the tested devices were equipment CR and the biggest source of noise for such equipment was the structural noise. One possible explanation for the b values mostly above 0,5 would be the fact that all digital systems, except CR systems, have the effects of structural noises removed almost entirely by-flat fielding operation, which is used to remove the influence of the anode effect and the sensitivity variation within and between the image plates. For DR systems, the power index stayed below 0.350 linking this result to more influence of electronic noise since these systems use the flat fielding operation.

Another explanation for this values it is the possible compensation in calibration of the systems, that employ high dosages in order to reduce noise.

Fig. 4 presents the dispersion of power index values obtained for each evaluated CR and DR mammography system. The minimum and maximum dispersions found are respectively: 0.141 and 1.203.

Table 7
Minimum and maximum values found for each thickness of PMMA in the CNR test.

Thickness of PMMA (cm)	Minimum value of relative CNR	Maximum value of relative CNR
2	63.9	347.5
3	101.3	285.3
4	74.6	1127
5	100	100
6	18.8	175.1
7	17.1	161.6

3.4. Image quality

The automated assessment of image quality is an important tool for quality control, avoiding the subjectivity of human evaluation. Such assessment should be performed when installing equipment, as well as annually or when there is any change in equipment (SEFM, 2012).

This study evaluated 62 images, of which 65% were considered of good quality. For the remaining 35%, the generated image did not allow the detection of the gold records through the software because the images had poor quality presenting low contrast (Table 9). The another ten images were not analyzed because the software displayed an error message. It is our belief that the error came from several factors, such as: improper positioning of the phantom; the phantom was cut showing the improper size of field in some images; error in the system and insufficient contrast provided by the system. For DR systems, an image was not evaluated for the reasons mentioned above, the other two systems had a good performance.

A study by Oliveira (Oliveira et al., 2007) of conventional mammography services found 54% of non-compliance to image quality. Dantas (2010), assessing automated image quality with the aid of the interpretation of the phantom CDMAM software (CDMAM Analyser Software V1.2), found a 43% non-compliance in Minas Gerais mammography services. It can be seen through this research a slight increase in image quality in mammography in Minas Gerais state.

3.5. Mean glandular dose

The mean glandular dose measurements were made for different thicknesses of PMMA (20–70 mm) to simulate the doses to which breasts of different thickness are subjected during mammograms using a digital system. Table 6 shows the cut-off for non-

Table 8
Uncertainties related to kerma measurements.

Sources of uncertainty	Value (%)	Probability distribution	Divisor	Standard uncertainty (u_i)	Type
Calibration	1.0	Normal (k)	2.00	0.50	B
Resolution	0.5	Rectangle	1.73	0.29	B
Energy dependency	5.0	Normal (k)	2.00	2.50	B
Angular dependence	0.5	Normal (k)	2.00	0.25	B
Position	0.3	Rectangle	1.73	0.17	B
Combined standard uncertainty (u_c)	2.58	Normal			
Expanded uncertainty (U)	**5.2**	(Probability ≈ 95%)		**Coverage factor (k)=2**	

compliance for the mean glandular dose.

The uncertainty assigned to the mean glandular dose measured with the solid-state dosimeter (Unfors Xi) was estimated. The components evaluated are shown in Table 8. Error propagation, as described in the Guide to the Expression of the Uncertainty in Measurement (GUM), was used for the estimation of all the components of the mean glandular dose that had expanded uncertainty with a confidence level of 95% and a coverage factor (k=2) (GUM, 1995).

For D_G of 20 mm thicknesses, it was observed an average value of 0.84 mGy. The lowest value found was 0.201 mGy and the highest of 3.6 mGy. Fourteen services obtained doses above the acceptable limit of 1.00 mGy. For D_G of 30 mm thicknesses, it was observed an average value of 1.3 mGy. The lowest value found was 0.3 mGy and the highest of 3.1 mGy. Fifteen services obtained doses above the acceptable limit of 1.5 mGy. For D_G of 40 mm thicknesses, it was observed an average value of 2.1 mGy. The lowest value found was 0.5 mGy and the highest of 6.7 mGy. Thirty services obtained doses above the acceptable limit of 2.00 mGy. For D_G of 50 mm thicknesses, it was observed an average value of 2.9 mGy. The lowest value found was 0.76 mGy and the highest of 12.06 mGy. Twenty-seven services obtained doses above the acceptable limit of 3.00 mGy. For D_G of 60 mm thicknesses, it was observed an average value of 4.1 mGy. The lowest value found was 0.8 mGy and the highest of 21.07 mGy. Twenty-three services obtained doses above the acceptable limit of 4.5 mGy. For D_G of 70 mm thicknesses, it was observed an average value of 5.6 mGy. The lowest value found was 1.9 mGy and the highest of 37.21 mGy. Fifteen services obtained doses above the acceptable limit of 6.5 mGy. This study found 44% of CR and DR mammography systems to be compliant for all evaluated thicknesses of PMMA (Table 9). It is worth noticing that one of the three DR systems evaluated obtained doses above the limits considered acceptable.

Table 10 shows the evaluation results for D_G in thicknesses from 20 to 70 mm PMMA compared to the results of Dantas (2010).

In comparison with the Dantas (2010) study, a decrease of 25% was observed in the percentage of compliance for D_G for all thicknesses of PMMA. It can also be noted that most of the evaluated facilities presented a significant increase in dose levels for all simulated breast thicknesses (Table 10).

Table 9
Summary of all results of the quality control test in 72 mammography systems assessed.

Test	Compliant %	Non compliant %
Linearity of the detector response	85	15
Contrast-to-noise ratio	10	90
Power index values (noise)	31	69
Image quality CDMAM	65	35
Mean glandular dose	44	56

A 2007 study by Oliveira (Oliveira et al., 2007) on conventional mammography services in Minas Gerais measured an average value of 1.32 mGy for D_G in a phantom 50 mm PMMA. Thus, comparing conventional mammography and CR mammography, for D_G, it appears that in the latter case the D_G received is around 119% higher.

The CR cassette is actually more attenuating than film cassettes, but that's not the main reason for such a drastic increase in dose, not even the tube wear.

This drastic increase in the dose may be explained by the dynamics range of each system. Conventional systems have a sigmoid dynamic range, being only linear in a small range of values.

From which, low and high dosages have small variations in the optical density of the image (D.O). Such systems have a significant variation only in the linear range of the curve. On the other hand, digital systems have a linear dynamic range such any dose change produce a variation in D.O. This characteristic makes it able to produce images with a suitable contrast level, to some extent, in any dose range for digital systems. In conventional systems it becomes impossible because low dosages produce and higher dosages produce no contrast image. However, digital images with low doses have a large amount of noise.

Note that digital systems were introduced in Brazil just changing the conventional to an computadorized processing without taking into account the performance of the systems working together.

What can be observed is that the services are calibrating the systems with high dosages in order to reduce noise and not lose images, the system calibration is being done indiscriminately at the expense of the dose the patient will receive, without considering the limitation of the conventional system. Another aspect worth mentioning is that there are a loss of information in the process of image scanning to the CR systems, so increasing the signal to noise ratio. As a result, there are a need to increase the dose so that the CNR became lower.

An evidence for this is the result in the noise test, where all CR systems obtained the structural noise as major component. The referred noise is dose-dependent.

The same fact is not observed in DR systems where all systems obtained the electronic noise as a major component, because this system cannot be adapted to the use of conventional mammography and has a linear dynamic range.

The mammography CR systems can be optimized and work properly. But the calibration has to be made so that the best image be performed with the lowest possible dose.

Moura et. al. (2014) measured D_G in patients with 4–6-cm compressed breast and glandularity of 50%, during the implementation of the projects RLA/9057 and 9067 (2007-09) in 53 institutions across Latin America, including Brazil, of which 33 used analog and 20 used digital equipment (equally divided between CR and DR). The results showed average D_G values for Brazil of 3.44 mGy (analog), 3.03 mGy (CR) and 3.46 mGy (DR) for MLO projections. For patient doses, the IAEA Basic Safety Standard Publication No. 115 has set a Diagnostic Reference Level (DRL) of 3 mGy for CC and MLO projections for PMMA phantom of 4.5 cm thickness. The UK, European and even IAEA Human Health Series (EC, 2006; NHSBSP, 2006, 2009), state an acceptable value of D_G 2.5 mGy and a target value of D_G 2 mGy for PMMA phantom of 4.5 cm thickness with equivalent breast thickness of 5.3 cm.

4. Conclusions

The linearity of the detector response to the CR and DR systems, in agreement with D_G, met the performance criteria

Table 10
D_G comparison between this study and Dantas (2010).

Thickness of PMMA (mm)	D_G (mGy) average for this study	D_G (mGy) average for Dantas (2010)	Percentage of increasing doses	Acceptable (SEFM, 2012)	Desirable (SEFM, 2012)
20	0.84	0.73	15	< 1.0	< 0.6
30	1.3	1.09	19	< 1.5	< 1.0
40	2.1	1.79	17	< 2.0	< 1.6
50	2.9	2.47	17	< 3.0	< 2.4
60	4.1	3.49	17	< 4.5	< 3.6
70	5.6	5.31	5	< 6.5	< 5.1

specified by SEFM (2012), with 85% compliance for the services evaluated. The evaluation of mammography images showed 65% compliance for the services evaluated, which represents an increase of almost 10% on the overall percentage in previous research by Dantas (2010), where services showed 57% compliance. Radiation levels to patient and image quality do not conform to regulations in many facilities.

90% of digital systems evaluated were non-compliant with the assessment of the contrast to noise ratio, also, 69% of digital systems evaluated were non-compliant with the assessment of the noise. Hence, there is a potential to optimize image quality and dose.

The correlation between image quality and dose is evaluated by means of the SNR and CNR. If there are good results at CNR, SNR and noise, then the image is of good quality and hence the CAE is working properly.

If the image is good even with low doses this means that the system is well calibrated. Getting good result of SNR and CNR with low doses is the optimum condition in a digital system.

That is not the case of the results found in this research. The higher doses found in this study compared to the doses obtained in conventional systems evaluated by Oliveira et al. (2007) are related to the calibration in appliances. It was observed that the services had been calibrated the systems with high dosages in order to overcome the limitation brought by noise.

Even if with a strict quality control program, the optimum dose level will never be reached if it do not have an adequate calibration of the entire mammographic system. And besides this, the majority of the mammography equipment has only one target filter combination Mo/Mo, that limit the techniques to be used.

This indicates that ongoing actions are needed to improve radiation dose and image quality for the early detection of breast cancer. According to the International Atomic Energy Agency (IAEA, 2005) there is the need to assess the state of optimization and protection in mammography in different countries, identifying points where action is needed and documenting improvement after corrective actions are put into practice.

The lessons learned from this exercise, already conducted in several countries, will give an insight into the range of practices, standard problems, optimization and further inferences about how optimization can be effective. In the same exercise conducted in six countries of Eastern Europe, useful insights and analysis were made, achieving an average reduction of 25% of the dose while maintaining image quality.

Based on the results from this research and the international recommendations, it is advisable to create a specific legislation for digital radiology in Brazil, probably by implementing regulations that determine the performance requirements of the service, part of the problems encountered could be solved. While this new legislation is not created, the services should pay attention to the constant optimization of their establishments, with training and periodic evaluations, seeking better integration between mammography systems / CR, through technical working together with in CR maintenance and technical maintenance of the mammography system calibration, and the proper functioning of DR systems. Not to mention the correct choice of radiographic techniques for radiology technicians according to the specifics of each patient's breast.

It is worth noting that internationally speaking, the only CR system accepted by the British program for Early Detection of Breast Cancer (NHSBSP, 2007) and by the Food and Drug Administration (FDA) is the CR system of Fuji Medical Systems Tokio (Japan) for meeting all the specifics required by the agencies with regard to image quality and dose.

Furthermore, it is also recommended, based on the results of this research, a review of the use of CR systems in Brazil and optimization of digital mammographic systems as a whole.

Acknowledgments

The authors (B. B. de Oliveira and F. Leyton) wish to acknowledge the support of the doctoral fellowship of the National Commission of Nuclear Energy, CNEN, and the Graduate Program in Science and Technology of Radiation, Minerals and Materials of the Nuclear Technology Development Center, CDTN. The authors are thankful to Foundation of support to Research of the State of Minas Gerais (FAPEMIG) (PPM), Higher Education Personnel Improvement Coordination (CAPES) and National Research Council (CNPq) (PQ) for the financial support. This work is part of the project INCT Radiation Metrology in Medicine.

References

Artinis, 2014. ⟨http://www.artinis.com/product/cdmam34_analyser⟩ (accessed 22.09.14).
Bick, U., Diekmann, F., 2009. Digital Mammography. Springer Verlag, Berlin.
Bouwman, R., et al., 2009. An alternative method for noise analysis using pixel variance as part of quality control procedures on digital mammography systems. Phys. Med. Biol. v.54 (n.22), 6809–6822.
Chevalier, M., Torres, R., 2010. Digital mammography. Rev. Fis. Med. 2010, 11–26.
CNES, 2014. Indicators from the National Registry of Health-CNES. Available at: ⟨http://cnes.datasus.gov.br/Mod_Ind_Equipamento.asp?VEstado=31⟩ (accessed 06.06.14).
Dance, D.R., et al., 1999. Breast dosimetry. Appl. Radiat. Isot. 1999 (50), 185–203.
Dance, D.R., et al., 2000. Additional factors for the estimation of mean glandular breast dose using UK mammography dosimetry protocol. Phys. Med. Biol. 45, 3225–3240.
Dantas, 2010. Dantas Marcelino Vicente de A. Dose glandular e controle de qualidade da imagem em serviços de mamografia com sistema de radiografia

computadorizada. 119 f. Dissertação (Mestrado em Ciência e Tecnologia das Radiações, Minerais e Materiais) – Centro de Desenvolvimento de Tecnologia Nuclear, Belo Horizonte.
EC (Commission of the European Communities), 2006. European Guidelines for Quality Assurance in Breast Cancer Screening and Diagnosis, 4th ed. European Commission, Office for Official Publications of the European Communities, Luxembourg.
GUM, 1995. BIPM, IEC, IFCC, ILAC, ISO, IUPAC, IUPAP and OIML 2008 Guide to the Expression of Uncertainty in Measurement. JCGM 100:2008, GUM 1995 with minor corrections.
IAEA (International Atomic Energy Agency), 2005. Optimization of the radiological protection of patients: Image Quality and Dose in mammography (coordinated research in Europe). IAEA, Vienna, p. 2005 (TECDOC, 1447).
ICRU (International commission on radiation units and measurements), 2009. Mammography - Assessment of Image Quality. Oxford, United Kingdom, ICRU REPORT 82.
INCA (Instituto Nacional De Câncer), 2014. Estimativa 2014: Incidência de câncer no Brasil. INCA, Rio de Janeiro, Brazil.
Mora, P., et al., 2014. Latin American dose survey results in mammography studies under IAEA programme: radiological protection of patients in medical exposures (TSA3). Radiat. Prot. Dosim. 163, 1–7.
NHSBSP, 2006. National Health Service Breast Screening Programmes. Commissioning and Routine Testing of Full Field Digital Mammography Systems. NHSBSP Equipment Report 0604. Version 2, September 2006, London, UK.
NHSBSP, 2007. National Health Service Breast Screening Programmes. Routine Quality Control Tests for Full Field Digital Mammography Systems. NHSBSP Equipment Report 0702, Version 1, February 2007, London, UK.
NHSBSP, 2009. National Health Service Breast Screening Programmes. Commissioning and Routine Testing of Full Field Digital Mammography Systems. NHSBSP Equipment Report 0604. Version 3, April 2009, London, UK.
Oliveira, B.B., et al., 2014. Mean glandular dose for different angles of the X-ray tube using different glandularity phantoms. Radiat. Phys. Chem. 95 (2014), 202–204.
Oliveira, M., et al., 2007. Average glandular dose and phantom image quality in mammography. Nucl. Instrum. Methods Phys. Res. A 580, 574–577.
Oliveira, M.A., et al., 2011. Assessment of glandular dose and image quality in mammography using computerised radiography employing a polymethylmetacrilate breast simulator. Radiat. Meas. 46, 2081–2085 2011.
Perry, N., et al., 2006. European Guidelines for Breast Cancer Screening and Diagnosis. Office for the Official Publications of the European Communities, Luxemburg.
SEFM (Sociedad Española De Fisica Medica), 2007. Sociedad Española De Fisica Medica, Protocolo de Control de Calidad en los sistemas digitales maograficos. Madrid.
SEFM (Sociedad Española De Fisica Medica), 2012. Protocolo Español de Control de Calidad en Radiodiagnóstico. Madrid.
Thijssen, M.A.O et al., 2006. Manual Contrast – Detail Phantom Artinis Cdmam Type 3.4. The Netherlands, 2006.